

## Designing Frequency Selective Filters Via the Use of Hyperbolic Tangent Functions

### Tanjant Hiperbolik Fonksiyonlar ile Frekans Seçici Süzgeç Tasarımı

Ahmet Tuğrul BAŞOKUR

Ankara Üniversitesi, Mühendislik Fakültesi, Jeofizik Mühendisliği Bölümü, Tandoğan, 06100 Ankara

Geliş (received) : 07 Aralık (December) 2010  
Kabul (accepted) : 24 Mart (March) 2011

#### ABSTRACT

A new parameterization of the hyperbolic tangent function is suggested for easy control of the width of the transition region between the limiting values of -1 and 1. The hyperbolic tangent function approaches the signum function as the suggested half-width parameter approaches zero. This permits definition of the rectangular function as the limiting case of a combination of two shifted hyperbolic tangent functions. Since all types of ideal frequency reject filter are derived from the rectangular function, the hyperbolic tangent window can also be used for the same purpose. The suggested filters are continuities in the whole space and provide an opportunity for easy control of the width of the passband, transition band and stopband through adjustment of the half-width parameter. A variety of examples are provided to instruct the design and application of one- and two-dimensional frequency reject filters. The formulation and examples are restricted to four types of filter, namely low-, band- and high-pass, and band-stopping filters. However, the results can easily be generalized for any type of frequency reject filter.

**Key Words:** Digital filter design, low-pass filters, band-pass filters, high-pass filters, band-stopping filters.

#### ÖZ

Tanjant hiperbolik fonksiyonu için -1 ve 1 limit değerleri arasında değişen geçiş bölgesi genişliğinin kolay denetimi amacı ile yeni bir parametreleştirme önerilmiştir. Önerilen yarı-genişlik parametresi sifıra yaklaştığında, tanjant hiperbolik fonksiyonu da işaret fonksiyonuna yaklaşmaktadır. Bu özellik, dikdörtgen fonksiyonun, iki kaymış tanjant hiperbolik fonksiyonunun bileşiminin limit durumu olarak tanımlanmasına izin verir. Bütün ideal frekans seçici süzgeçler dikdörtgen fonksiyondan türetildiğinden, hiperbolik tanjant fonksiyonu da aynı amaç için kullanılabilir. Önerilen süzgeçler tüm uzayda sürekli olup, geçirme-aralığı, geçiş-aralığı ve durdurma-aralığının genişliklerinin denetlenmesini olanaklı kılar. Bir- ve iki-boyutlu frekans seçici süzgeçlerin tasarımı ve uygulaması için örnekler verilmiştir. Bağıntılar ve örnekler, alçak-geçişli, aralık-geçişli, yüksek-geçişli ve aralık-durdurucu süzgeçler ile kısıtlı tutulmakla birlikte, herhangi bir süzgeç türüne kolaylıkla genelleştirilebilir.

**Anahtar Kelimeler:** Sayısal süzgeç tasarımı, alçak-geçişli süzgeçler, aralık-geçişli süzgeçler, yüksek-geçişli süzgeçler, aralık-durdurucu süzgeçler.

---

A.T. Başokur

E-mail: basokur@eng.ankara.edu.tr

## INTRODUCTION

Digital filters have specific importance to geophysical data processing because the signal/noise ratio has to be increased before the application of inversion and other types of data interpretation. Linear filter theory is based on the definition of a proper window function in the frequency domain of a low-pass filter. Other filter types such as band-pass, high-pass and band-stopping can be derived from a basic low-pass filter window through the use of algebraic operations. Several window functions have been suggested for the design of digital filters, each with their own advantages and disadvantages. To this author's knowledge, the hyperbolic tangent (HT) window was first defined by Johansen and Sorensen (1979) and is used for the truncation of filter characteristics at the Nyquist frequency in order to compute a filter coefficient set for the estimation of the Hankel transform of a discrete data set. This window provides a well-behaved transition within the frequency domain with which to truncate the spectrum, thus yielding a less oscillating interpolation function in the time domain for discrete Hankel transform computations (Christensen, 1990; Sorensen and Christensen, 1994). Başokur (1998) adapted the HT window for the description of one-dimensional frequency reject filters, which have subsequently been used in various applications. For example, Domaradzki and Carati (2007a, 2007b) were used these frequency rejected filters in the analysis of nonlinear interactions and energy transfer in turbulence. In biology, Opalka et al (2010) used the filter described by Başokur(1998) for the enhancement of cryo-images of *Eco* RNA polymerase particles. The HT filters were embedded into SPARX software that is used to process the images obtained from the cryo-electron microscopy (see Baldwin and Penczek, 2007). These applications in varied fields indicate a need for the further development of HT filters for easy control of the transition band. This paper suggests new half-width parameters for the direct solution of this problem. Additionally, the basic expressions for the box-shaped and radially-symmetric two-dimensional HT filters are derived both in the time and frequency domains. The computer programs and related

supplementary material that can be requested from the author enable both the processing of field data and the production of artificial data for testing the success of filter design. The latter is also useful for educational purposes.

## ONE-DIMENSIONAL DIGITAL FILTERS

### Low-pass filter design

An ideal low-pass filter should reject all frequencies higher than a cutoff frequency of  $f_L$ . The regions corresponding to frequencies lower and higher than the cutoff frequency are called passband and stopband, respectively. In practice however, a gradational attenuation of amplitudes is allowed around the cutoff frequency. This transition band permits the frequency response transition from passband to stopband. One of the proper functions for this type of filter construction is the P-function, derived in Appendix A from two shifted HT functions. Rewriting equation (A12) in the frequency domain gives the frequency response of a low-pass filter:

$$H_L(f) = P(f) = \frac{1}{2} \left\{ \tanh \left[ \frac{2(f + f_L)}{r_L} \right] - \tanh \left[ \frac{2(f - f_L)}{r_L} \right] \right\}, \quad (1)$$

where  $r_L$  denotes the half-width of the transition band. Figure 1a provides examples of frequency responses calculated for a variety of transition bands that share the same cutoff frequency. The use of the P-function as a frequency response for low-pass filters provides an efficient tool to control the width of the transition band. The amplitude of frequency response is equal to 0.5 at the cutoff frequency. It almost equals to unity and zero at the frequencies of  $(f_L - r_L)$  and  $(f_L + r_L)$ , respectively.

If the filter process is applied to digital data it is then necessary to multiply the frequency response by a rectangular function whose height and width are equal to the sampling rate ( $\Delta t$ ) and its reciprocal, respectively (see for example Ghosh, 1971; Basokur, 1983). Since the Nyquist frequency ( $f_N$ ) is defined as half of the reciprocal of the sampling rate, the filter spectrum is given as follows:

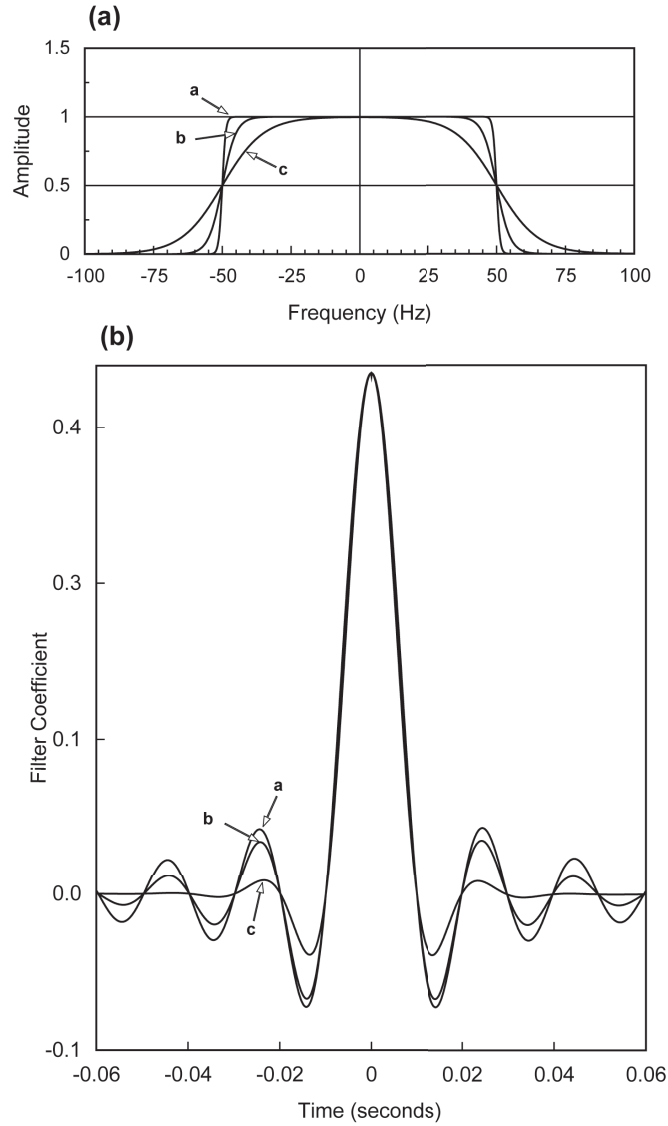


Figure 1. Low-pass filter responses in the frequency domain with varying transition-band widths of  $r_L=2.5$  Hz (a),  $r_L=10$  Hz (b) and  $r_L=30$  Hz (c) calculated for a cutoff frequency of 50 Hz (upper panel) and the corresponding filter coefficients in the time domain (lower panel).

Şekil 1. Frekans bölgesinde değişen geçiş-aralıkları  $r_L=2.5$  Hz (a),  $r_L=10$  Hz (b) ve  $r_L=30$  Hz (c) için 50 Hz kesme frekanslı alçak-geçişli süzgeç yanıtları (üstte) ve bunlara karşılık gelen zaman bölgesi süzgeç katsayıları (altta).

$$B_L(f) = \Delta t \text{rect}(1/2\Delta t) H_L(f) = \Delta t \text{rect}(f_N) H_L(f) \quad (2)$$

The Nyquist frequency is always greater than the cutoff frequency and consequently, for a low-pass filter, the multiplication of frequency response by the rectangular function can only result in the multiplication of the frequency response by the sampling rate:

$$B_L(f) = \frac{\Delta t}{2} \left\{ \tanh \left[ \frac{2(f + f_L)}{r_L} \right] - \tanh \left[ \frac{2(f - f_L)}{r_L} \right] \right\} \quad (3)$$

The first step of the filtering operation in the frequency domain is to perform a discrete Fourier transform of the sampled data. The

transformed data is then multiplied by the filter spectrum, and finally the inverse Fourier transform applied to the outcome of this multiplication yields the filtered data in the time domain.

Since multiplication in the frequency domain is equivalent to convolution in the time domain, as an alternative procedure digital filtering can also be performed by a convolution of the measured data with the inverse transform of the filter spectrum. The time domain convolution operator is known as a 'filter coefficient' that can be easily obtained from the transform pair of (A15) by using the symmetry property of the Fourier transform:

$$b_L(t) = \frac{\pi r_L}{4f_N} \frac{\sin(2\pi f_L t)}{\sinh(\pi^2 r_L t/2)} \leftrightarrow B_L(f) \quad (4)$$

where the double arrow denotes the Fourier transform pair.  $B_L(f)$  approaches the ideal low-pass frequency response as the half-width of the transition band approaches zero. Correspondingly,  $b_L(t)$  approaches the *sinc*-response in the time domain (see equation A17 in the Appendix) since  $\sinh(x) \cong x$  for small arguments:

$$\lim_{r_L \rightarrow 0} \frac{\pi r_L}{4f_N} \frac{\sin(2\pi f_L t)}{\sinh(\pi^2 r_L t/2)} = \frac{\sin(2\pi f_L t)}{2\pi f_N t} \leftrightarrow \lim_{r_L \rightarrow 0} B(f) = \Delta t \text{rect}(f_L) \quad (5)$$

For the above reason, ideal filters can be considered as a special case of HT filters, and it is sufficient to supply an extremely small transition band for the construction of an ideal filter. The filter coefficients defined in expression (4) can be written in a more familiar form by using the smoothness parameter of Johansen and Sorensen (1979) (see (A16)):

$$b_L(t) = \frac{\alpha f_L}{f_N} \frac{\sin(2\pi f_L t)}{\sinh(2\pi \alpha f_L t)} \quad (6)$$

where

$$\alpha = \frac{\pi r_L}{4f_L} \quad (7)$$

The limits of (4), (6) and the *sinc*-response approach the same numerical value for time zero:

$$b_L(0) = \frac{f_L}{f_N} \quad (8)$$

As an analogy to the term *sinc*-response, Johansen and Sorensen (1979) described a similar form of (6) as the *sinsh*-response. In practice, the use of a newly-derived parameter ( $r_L$ ) is more helpful in controlling the half-width of the transition band compared with the smoothness coefficient ( $\alpha$ ) given by Johansen and Sorensen (1979). Despite this difference, equation (4) will hereupon be also referred to as the *sinsh*-response. Figure 1b shows *sinsh*-responses obtained from equation (4) whose filter spectra are shown in the upper panel of Figure 1. The oscillations of the filter coefficients decrease as the transition-band of the filters becomes wider in the frequency domain. This property provides an opportunity to design relatively short filters in the time domain. Some examples of the application of the filtering operation in the time and frequency domains will be presented in the application section.

### Band-pass filter design

An ideal band-pass filter removes all information except the frequency band between low- and high-cutoff frequencies. Band-pass filters can be obtained from the subtraction of two low-pass filters with different cutoff frequencies. Figure 2 describes the construction of a band-pass filter. The half-width of transition bands around low- ( $f_L$ ) and high-cutoff ( $f_H$ ) frequencies can be freely selected, permitting the independent adjustment of the slope in the transition band. Rewriting (1) for two different cutoff frequencies and transition-band widths, and subtracting one from the other yields

$$H_B(f) = \frac{1}{2} \left\{ \begin{array}{l} \tanh\left[\frac{2(f+f_H)}{r_H}\right] - \tanh\left[\frac{2(f-f_H)}{r_H}\right] \\ - \tanh\left[\frac{2(f+f_L)}{r_L}\right] + \tanh\left[\frac{2(f-f_L)}{r_L}\right] \end{array} \right\} \quad (9)$$

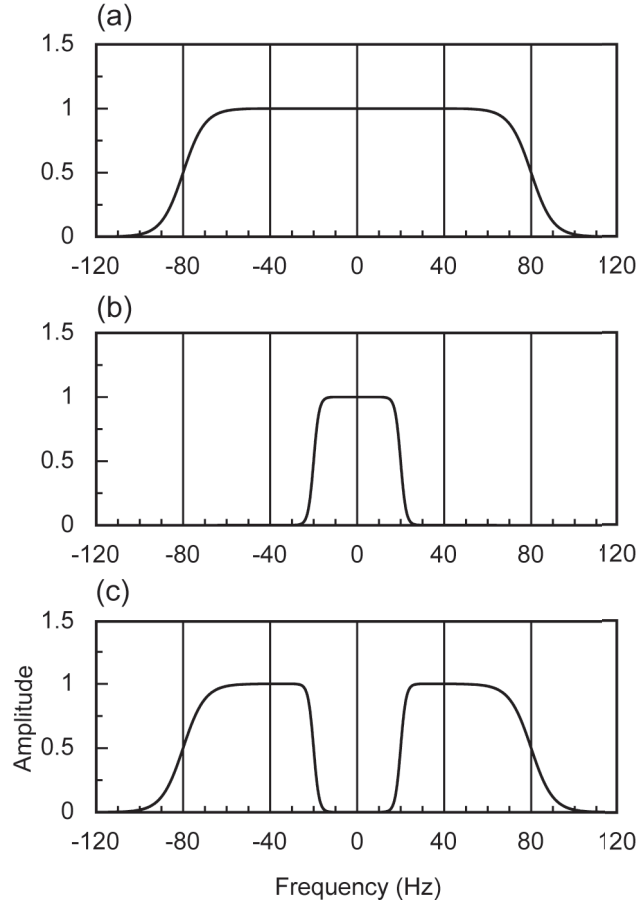


Figure 2. Construction of a band-pass filter by the subtraction of two low-pass filters. The half-width values are  $r_H = 20$  Hz (a) and  $r_L = 5$  Hz (b), corresponding to the half-width of the transition-band at the high-end and low-end frequency sides, respectively. The high and low cutoff frequencies are equal to 80 and 20 Hz. The final band-pass filter presented in (c) exhibits different slopes and widths in the low and high transition-band frequencies.

Şekil 2. İki alçak-geçişli süzgecin birbirinden çıkarılması ile aralık-geçişli süzgecin oluşturulması. Yarı-genişlik değerleri  $r_H = 20$  Hz (a) ve  $r_L = 5$  Hz (b), geçiş bölgesinin sırası ile yüksek ve düşük kesme bölgelerine karşılık gelmektedir. Yüksek ve düşük kesme frekansları 80 ve 20 Hz değerlerine eşittir. Elde edilen aralık-geçişli süzgecin, düşük ve yüksek geçirme-aralıklarında farklı eğim ve genişliği bulunmaktadır.

where  $r_L$  and  $r_H$  correspond to the half-widths of transition-bands at the low- and high-cutoff frequencies. The filter spectrum can be derived from the multiplication of the frequency response (equation 9) by the rectangular function. This yields

$$B_B(f) = \Delta t \text{rect}(1/2\Delta t) H_B(f) = \Delta t H_B(f) \quad (10)$$

The inverse Fourier transform of the filter spectrum results in the following weight coefficients in the time domain:

$$b_B(t) = \frac{\pi}{4f_N} \left[ \frac{r_H \sin(2\pi f_H t)}{\sinh(\pi^2 r_H t / 2)} - \frac{r_L \sin(2\pi f_L t)}{\sinh(\pi^2 r_L t / 2)} \right] \quad (11)$$

$$b_B(t) = \frac{f_H}{f_N} \frac{\alpha_H \sin(2\pi f_H t)}{\sinh(2\pi \alpha_H f_H t)} - \frac{f_L}{f_N} \frac{\alpha_L \sin(2\pi f_L t)}{\sinh(2\pi \alpha_L f_L t)} \quad (12)$$

$$b_B(0) = (f_H - f_L) / f_N \quad (13)$$

with  $\alpha_L = \pi r_L / 4f_L$  and  $\alpha_H = \pi r_H / 4f_H$ .

The sample values of the above expression give the desired filter coefficients. Other properties of the band-pass filter are the same as those of the low-pass filter.

### High-Pass Filter Design

All frequencies higher than the cutoff frequency of  $f_H$  should be passed by an ideal high-pass filter. The construction of a high-pass HT frequency response and spectrum is illustrated in Figure 3. The frequency response can be derived from the subtraction of a low-pass frequency response from unity:

$$H_H(f) = 1 - \frac{1}{2} \left\{ \tanh \left[ \frac{2(f + f_H)}{r_H} \right] - \tanh \left[ \frac{2(f - f_H)}{r_H} \right] \right\} \quad (14)$$

where  $f_H$  and  $r_H$  correspond to the high-cut-off frequency and the half-width of the frequency response at the transition-band (Figure 3c). The multiplication of the frequency response by the rectangular function yields the filter spectrum (Figure 3d):

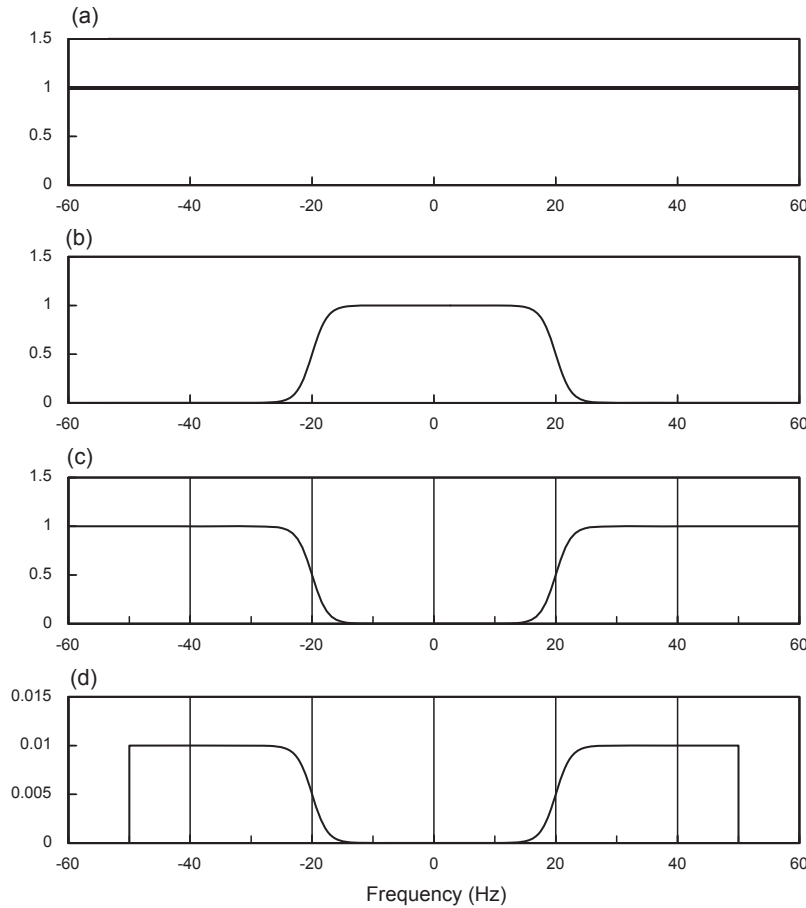


Figure 3. Development of the filter spectrum for a high-pass filter. A low-pass filter response (b) is subtracted from unity (a) to obtain a high-pass frequency response function (c). A multiplication of the filter response by the rectangular function, whose height and width are equal to the sampling rate, produces the final filter spectrum (d).  $f_H = 20$  Hz,  $f_N = 50$  Hz,  $\Delta t = 0.01$  sec,  $r_H = 5$  Hz.

Şekil 3. Yüksek-geçişli süzgecin geliştirilmesi. Yüksek-geçişli süzgeç (c) elde etmek amacı ile alçak-geçişli süzgeç yanıtı (b), birim değerden (a) çıkartılır. Süzgeç yanıtının, yüksekliği ve genişliği örnekleme aralığına eşit olan dikdörtgen fonksiyon ile çarpımı süzgeç izgesini üretir (d).  $f_H = 20$  Hz,  $f_N = 50$  Hz,  $\Delta t = 0.01$  sn,  $r_H = 5$  Hz.

$$B_H(f) = \Delta t \operatorname{rect}(f_N) H_H(f),$$

$$B_H(f) = \Delta t \operatorname{rect}(f_N) - \frac{\Delta t}{2} \left\{ \tanh \left[ \frac{2(f+f_H)}{r_H} \right] - \tanh \left[ \frac{2(f-f_H)}{r_H} \right] \right\} \quad (15)$$

The inverse Fourier transform of the filter spectrum will result in the filter weights in the time domain:

$$b_H(t) = \frac{\sin(2\pi f_N t)}{2\pi f_N t} - \frac{\pi r_H}{4f_N} \frac{\sin(2\pi f_H t)}{\sinh(\pi^2 r_H t/2)} \quad (16)$$

If the filter coefficients are calculated for the abscissa values  $t = \bar{F}n \cdot \Delta t$ , the numerical values of  $\sin(2\pi f_N t)$ , except the origin, then become zero:

$$b_H(t) = -\frac{\pi r_H}{4f_N} \frac{\sin(2\pi f_H t)}{\sinh(\pi^2 r_H t/2)} = -\frac{\alpha f_H}{f_N} \frac{\sin(2\pi f_H t)}{\sinh(2\pi \alpha f_H t)} \quad t = \bar{F}n \cdot \Delta t; n \neq 0 \quad (17)$$

with  $\alpha = \pi r_H / 4f_H$ . The weight coefficients at the centre of the filter can be found by examining the limit of equation (16) as follows:

$$b_H(0) = 1 - f_H / f_N. \quad (18)$$

### Band-stopping filters

An ideal band-stopping filter rejects frequencies within a predefined frequency band. These types of filter are obtained by a summation of low-pass and high-pass filters whose cutoff frequencies are  $f_L$  and  $f_H$ , respectively. The sum of expressions (1) and (14) yields

$$H_S(f) = \frac{1}{2} \left\{ \tanh \left[ \frac{2(f+f_L)}{r_L} \right] - \tanh \left[ \frac{2(f-f_L)}{r_L} \right] \right\} + 1 - \frac{1}{2} \left\{ \tanh \left[ \frac{2(f+f_H)}{r_H} \right] - \tanh \left[ \frac{2(f-f_H)}{r_H} \right] \right\} \quad (19)$$

The filter spectrum can be obtained by multiplying the frequency response by the rectangular function:

$$B_S(f) = \Delta t \operatorname{rect}(f_N) + \frac{\Delta t}{2} \left\{ \begin{aligned} &\tanh \left[ \frac{2(f+f_L)}{r_L} \right] - \tanh \left[ \frac{2(f-f_L)}{r_L} \right] \\ & - \tanh \left[ \frac{2(f+f_H)}{r_H} \right] + \tanh \left[ \frac{2(f-f_H)}{r_H} \right] \end{aligned} \right\} \quad (20)$$

The inverse Fourier transform of the filter spectrum yields the desired filter coefficients in the time domain:

$$b_S(t) = \frac{\sin(2\pi f_N t)}{2\pi f_N t} + \frac{\pi}{4f_N} \left[ \frac{r_L \sin(2\pi f_L t)}{\sinh(\pi^2 r_L t/2)} - \frac{r_H \sin(2\pi f_H t)}{\sinh(\pi^2 r_H t/2)} \right] \quad (21)$$

The first term in the above equation becomes zero, except at the origin, if the filter coefficients are calculated for abscissa values equal to  $t = \bar{F}n \cdot \Delta t$ :

$$b_S(t) = \frac{\pi}{4f_N} \left[ \frac{r_L \sin(2\pi f_L t)}{\sinh(\pi^2 r_L t/2)} - \frac{r_H \sin(2\pi f_H t)}{\sinh(\pi^2 r_H t/2)} \right] \quad t = \bar{F}n \cdot \Delta t; n \neq 0 \quad (22)$$

The limiting value for the zero abscissa point can be derived from (21) as follows:

$$b_S(0) = 1 + \frac{f_L}{f_N} - \frac{f_H}{f_N} = 1 - \frac{f_H - f_L}{f_N} \quad (23)$$

An alternative form for expression (22) can be given as

$$b_S(t) = \alpha_L \frac{f_L}{f_N} \frac{\sin(2\pi f_L t)}{\sinh(2\pi \alpha_L f_L t)} - \alpha_H \frac{f_H}{f_N} \frac{\sin(2\pi f_H t)}{\sinh(2\pi \alpha_H f_H t)} \quad t = \bar{F}n \cdot \Delta t; n \neq 0 \quad (24)$$

with  $\alpha_L = \pi r_L / 4f_L$  and  $\alpha_H = \pi r_H / 4f_H$ .

## TWO-DIMENSIONAL FILTERS

### Two-dimensional box-shaped filters

The measured data can be dependent on both time and distance variables ( $t$ - $x$  domain) as is the case in seismic. The domain of Fourier transformed data corresponding to distance is the spatial frequency (wavenumber), which has a dimension defined by the number of cycles per

unit distance. The 2D Fourier transform of the measured data provides a frequency-wavenumber representation ( $f$ - $k$  domain). In such cases, the cutoff wavenumber and cutoff frequency are likely to differ from each other numerically and as a consequence the frequency response will resemble a box-shaped function that can be expressed as the multiple of one frequency and one wavenumber filter; each being a function of either frequency or wavenumber:

$$H_{2L}(f, k) = H_{2L}(f) H_{2L}(k), \quad (25)$$

where

$$H_{2L}(f) = \frac{1}{2} \left\{ \tanh \left[ \frac{2(f + f_L)}{r_{Lf}} \right] - \tanh \left[ \frac{2(f - f_L)}{r_{Lf}} \right] \right\} \quad (26)$$

$$H_{2L}(k) = \frac{1}{2} \left\{ \tanh \left[ \frac{2(k + k_L)}{r_{Lk}} \right] - \tanh \left[ \frac{2(k - k_L)}{r_{Lk}} \right] \right\} \quad (27)$$

$H_{2L}(f)$  and  $H_{2L}(k)$  represent one directional frequency and wavenumber filters, respectively, and  $r_{Lf}$  and  $r_{Lk}$  are the half-widths of the

transition-bands corresponding to cutoff frequency ( $f_L$ ) and cutoff wavenumber ( $k_L$ ). Figures 4a and 4b show one directional frequency and wavenumber filters that are perpendicular to each other. The multiplication of these one directional filters produces a box-shaped two-dimensional filter as shown in Figure 4c. Another example of the frequency response of a 2D box-shaped low-pass filter is illustrated in Figure 5a for comparison with the responses of other types of 2D filter. The derived equations also provide the possibility for one directional filtering of a 2D data set. For example, the filter operation can be carried out in only one direction by equating either (26) or (27) with the unity in equation (25).

A two-dimensional box-shaped band-pass frequency filter can be produced by the subtraction of two low-pass filters whose cut-off frequencies and wavenumbers are  $(f_H; k_H)$  and  $(f_L; k_L)$ , respectively:

$$H_{2B}(f, k) = H_{2L}(f, k, f_H, k_H) - H_{2L}(f, k, f_L, k_L) \quad (28)$$

which can also be written as

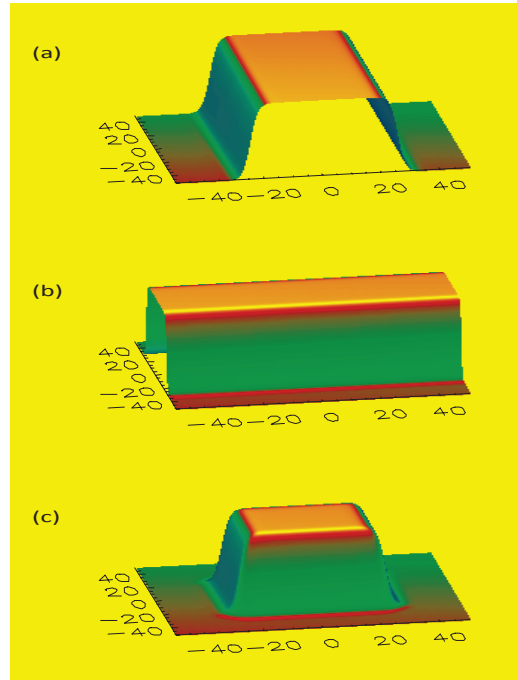


Figure 4. Development of a two-dimensional box-shaped filter by the multiplication of two one-directional filters.

Şekil 4. İki-boyutlu kutu-biçimli süzgecin iki adet tek-yönlü süzgecin çarpımından elde edilmesi.

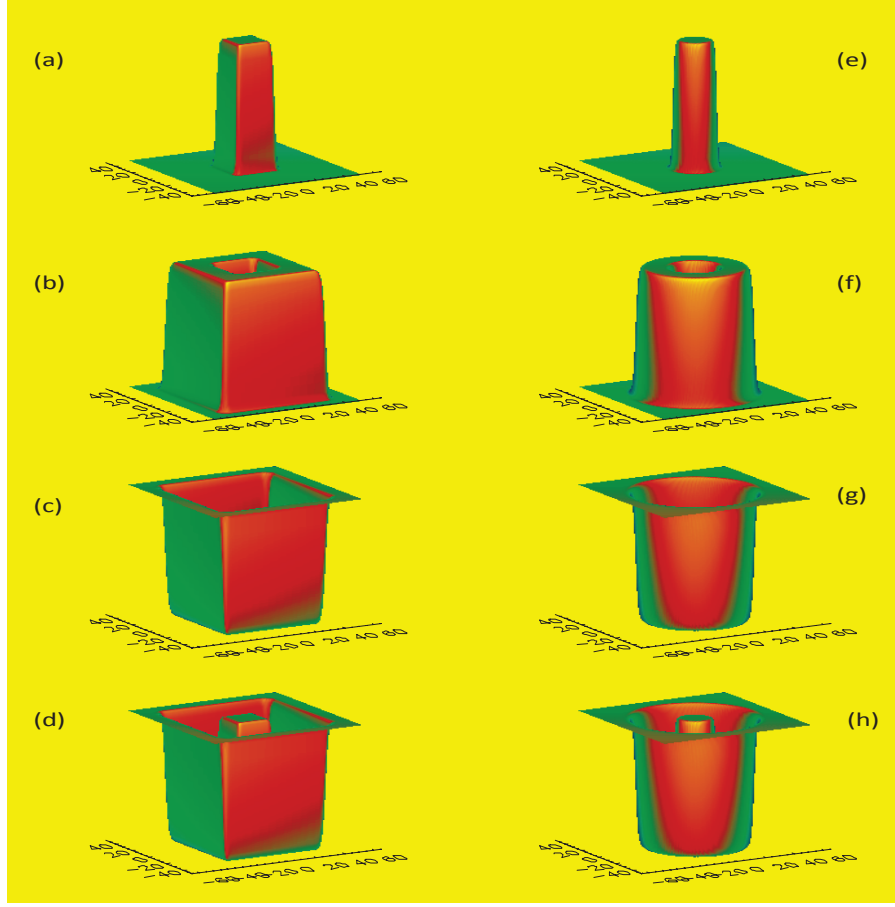


Figure 5. Frequency responses of two-dimensional box-shaped (left panel, a, b, c and d) and radially symmetric filters (right panel, e, f, g and h). The low and high cutoff frequencies are 13 and 35 Hz, with corresponding half-widths equal to 2 and 3 Hz, respectively.

Şekil 5. İki-boyutlu kutu-biçimli (sol panel, a, b, c ve d) ve ışınsal bakışimli (sağ panel, e, f, g ve h) süzgeç yanıtları. 13 ve 35 Hz alçak ve yüksek kesme frekansları değerlerine, sırası ile 2 ve 3 Hz yarı-genişlik değerleri karşılık gelmektedir.

$$H_{2B}(f, k) = H_{2L}(f, f_H) H_{2L}(k, k_H) - H_{2L}(f, f_L) H_{2L}(k, k_L) \quad (29)$$

where

$$H_{2L}(f, f_H) = \frac{1}{2} \left\{ \tanh \left[ \frac{2(f + f_H)}{r_{Hf}} \right] - \tanh \left[ \frac{2(f - f_H)}{r_{Hf}} \right] \right\} \quad (30)$$

$$H_{2L}(k, k_H) = \frac{1}{2} \left\{ \tanh \left[ \frac{2(k + k_H)}{r_{Hk}} \right] - \tanh \left[ \frac{2(k - k_H)}{r_{Hk}} \right] \right\} \quad (31)$$

$$H_{2L}(f, f_L) = \frac{1}{2} \left\{ \tanh \left[ \frac{2(f + f_L)}{r_{Lf}} \right] - \tanh \left[ \frac{2(f - f_L)}{r_{Lf}} \right] \right\} \quad (32)$$

$$H_{2L}(k, k_L) = \frac{1}{2} \left\{ \tanh \left[ \frac{2(k + k_L)}{r_{Lk}} \right] - \tanh \left[ \frac{2(k - k_L)}{r_{Lk}} \right] \right\} \quad (33)$$

In the above expressions,  $r$  denotes the half-width of the corresponding transition-band. Figure 5b shows a 2D box-shaped band-pass filter. The low-end frequency of the filter pass-band and half-width of the transition band on the low-end frequency side are 13 and 2 Hz, respectively, while the high-end frequency and corresponding half-width are 35 and 3 Hz. The same numerical values are used for the wave-number filter so that multiplication of the filters produces a square-shaped 2D band-pass filter.

A 2D high-pass frequency response can be constructed by the subtraction from unity of a low-pass frequency response whose cutoff frequency and wavenumber are equal to  $f_H$  and  $k_H$ , respectively:

$$H_{2H}(f, k) = 1 - H_{2H}(f) H_{2H}(k) \quad (34)$$

where

$$H_{2H}(f) = \frac{1}{2} \left\{ \tanh \left[ \frac{2(f + f_H)}{r_{Hf}} \right] - \tanh \left[ \frac{2(f - f_H)}{r_{Hf}} \right] \right\} \quad (35)$$

$$H_{2H}(k) = \frac{1}{2} \left\{ \tanh \left[ \frac{2(k + k_H)}{r_{Hk}} \right] - \tanh \left[ \frac{2(k - k_H)}{r_{Hk}} \right] \right\} \quad (36)$$

$r_{Hf}$  and  $r_{Hk}$  are the half-widths of transition-bands corresponding to a cutoff frequency of  $f_H$  and a wavenumber of  $k_H$ . Figure 5c shows a box-shaped high-pass filter obtained from the subtraction of a low-pass filter from unity. The cutoff frequencies and half-width values in both directions are equal to 35 and 3 Hz, respectively.

Any other type of filter can be developed by using two or more of the above-mentioned three basic low-, band- and high-pass filters. For example, a band-stopping filter can be produced from the sum of low- and high-pass filters. Figure 5d shows a band-stopping filter obtained from the sum of the low- and high-pass filters illustrated in Figures 5a and 5c, respectively.

The filter spectra of the above-mentioned filters can be calculated via the multiplication of the frequency response by two 2D rectangular functions whose widths are equal to the Nyquist frequency and wavenumber, respectively. The heights of the rectangular functions should be equal to half the reciprocal of the Nyquist frequency and wavenumber, respectively. The spectrum of any specific filter can then be obtained as follows:

$$B(f, k) = \frac{1}{2f_N} \text{rect}(f_N) - \frac{1}{2k_N} \text{rect}(k_N) H(f, k),$$

$$B(f, k) = \Delta t \text{rect} \left\{ \frac{1}{2\Delta t} \right\} \Delta x \text{rect} \left\{ \frac{1}{2\Delta x} \right\} H(f, k) \quad (37)$$

Since the cutoff values of all low-pass filters are always less than the Nyquist frequency and wavenumber, the multiplication in equation (37) reduces to

$$B_{2L}(f, k) = \Delta t \Delta x H_{2L}(f) H_{2L}(k) \quad (38)$$

The equation for a band-pass filter can be derived as follows:

$$B_{2B}(f, k) = \Delta t \Delta x \{ H_{2L}(f, k, f_H, k_H) - H_{2L}(f, k, f_L, k_L) \} \quad (39)$$

However, the rectangular function remains in the high-pass filter equation derived from (34) and (37):

$$B_{2H}(f, k) = \Delta t \text{rect}(f_N) \Delta x \text{rect}(k_N) - \Delta t \Delta x H_{2H}(f) H_{2H}(k) \quad (40)$$

2D box-shaped filters can also be designed in the time domain. The inverse Fourier transforms of the filter spectra provide the desired filter coefficients in the  $t$ - $x$  domain. The low-pass filter coefficients can then be calculated from the inverse Fourier transform of equation (38):

$$b_{2L}(t, x) = \left[ \alpha_t \frac{\alpha_x f_L}{f_N} \frac{\sin(2\pi f_L t)}{\sinh(2\pi \alpha_x f_L t)} \right] \left[ \frac{\alpha_x k_L}{k_N} \frac{\sin(2\pi k_L x)}{\sinh(2\pi \alpha_x k_L x)} \right] \quad t = \bar{n} \Delta t, \quad x = \bar{m} \Delta x \quad (41)$$

where  $\alpha_t = \pi r_{Lf} / 4f_L$  and  $\alpha_x = \pi r_{Lk} / 4k_L$ .

The limiting values of filter coefficients for zero values of time and spatial variables can be written as

$$b_{2L}(0, x) = \frac{f_L}{f_N} \frac{\alpha_x k_L}{k_N} \frac{\sin(2\pi k_L x)}{\sinh(2\pi \alpha_x k_L x)} \quad t = 0, \quad x = \bar{m} \Delta x \quad (42)$$

$$b_{2L}(t, 0) = \alpha_t \frac{f_L}{f_N} \frac{\sin(2\pi f_L t)}{\sinh(2\pi \alpha_t f_L t)} \frac{k_L}{k_N} \quad t = \bar{n} \Delta t, \quad x = 0 \quad (43)$$

$$b_{2L}(0, 0) = \frac{f_L}{f_N} \frac{k_L}{k_N}. \quad (44)$$

The filter coefficients for the band-pass filter can be derived using the subtraction of two low-pass filters, namely

$$b_{2B}(t, x) = b_{2L}(t, x, f_H, k_H) - b_{2L}(t, x, f_L, k_L) \quad (45)$$

where

$$b_{2L}(t, x, f_H, k_H) = \left[ \alpha_{fH} \frac{f_H}{f_N} \frac{\sin(2\pi f_H t)}{\sinh(2\pi \alpha_{fH} f_H t)} \right] \left[ \alpha_{kH} \frac{k_H}{k_N} \frac{\sin(2\pi k_H x)}{\sinh(2\pi \alpha_{kH} k_H x)} \right] \quad (46)$$

$$b_{2L}(t, x, f_L, k_L) = \left[ \alpha_{fL} \frac{f_L}{f_N} \frac{\sin(2\pi f_L t)}{\sinh(2\pi \alpha_{fL} f_L t)} \right] \left[ \alpha_{kL} \frac{k_L}{k_N} \frac{\sin(2\pi k_L x)}{\sinh(2\pi \alpha_{kL} k_L x)} \right] \quad (47)$$

The subscripts of the  $\alpha$  coefficients indicate the relevant variables and cutoff values. The limiting values of the above expressions can be obtained by assigning zero values to the corresponding variables:

$$b_{2B}(0, x) = \frac{f_H}{f_N} \frac{\alpha_{kH} k_H}{k_N} \frac{\sin(2\pi k_H x)}{\sinh(2\pi \alpha_{kH} k_H x)} - \frac{f_L}{f_N} \frac{\alpha_{kL} k_L}{k_N} \frac{\sin(2\pi k_L x)}{\sinh(2\pi \alpha_{kL} k_L x)} \quad (48)$$

$$b_{2B}(t, 0) = \frac{\alpha_{fH} f_H}{f_N} \frac{\sin(2\pi f_H t)}{\sinh(2\pi \alpha_{fH} f_H t)} \frac{k_H}{k_N} - \frac{\alpha_{fL} f_L}{f_N} \frac{\sin(2\pi f_L t)}{\sinh(2\pi \alpha_{fL} f_L t)} \frac{k_L}{k_N} \quad (49)$$

$$b_{2B}(0, 0) = \frac{f_H k_H - f_L k_L}{f_N k_N} \quad (50)$$

In a similar way, the filter coefficients of a high-pass filter can be derived from the inverse transform of (40) that gives

$$b_{2H}(t, x) = b_{2L}(t, x, f_N, k_N) - b_{2L}(t, x, f_H, k_H) \quad (51)$$

where

$$b_{2L}(t, x, f_N, k_N) = \frac{\sin(2\pi f_N t)}{2\pi f_N t} \frac{\sin(2\pi k_N x)}{2\pi k_N x} \quad (52)$$

$$b_{2L}(t, x, f_H, k_H) = \frac{\alpha_{fH} f_H}{f_N} \frac{\sin(2\pi f_H t)}{\sinh(2\pi \alpha_{fH} f_H t)} \frac{\alpha_{kH} k_H}{k_N} \frac{\sin(2\pi k_H x)}{\sinh(2\pi \alpha_{kH} k_H x)} \quad (53)$$

Equation (52) is always zero, except at points where  $t=0$ ;  $x=0$  and it becomes equal to unity. Accordingly, the filter coefficients of a high-pass filter can be computed from the following equations:

$$b_{2H}(t, x) = - \frac{\alpha_{fH} f_H}{f_N} \frac{\sin(2\pi f_H t)}{\sinh(2\pi \alpha_{fH} f_H t)} \frac{\alpha_{kH} k_H}{k_N} \frac{\sin(2\pi k_H x)}{\sinh(2\pi \alpha_{kH} k_H x)} \quad t \neq 0, x \neq 0 \quad (54)$$

$$b_{2H}(0, x) = - \frac{f_H}{f_N} \frac{\alpha_{kH} k_H}{k_N} \frac{\sin(2\pi k_H x)}{\sinh(2\pi \alpha_{kH} k_H x)} \quad t = 0, x \neq 0 \quad (55)$$

$$b_{2H}(t, 0) = - \frac{\alpha_{fH} f_H}{f_N} \frac{\sin(2\pi f_H t)}{\sinh(2\pi \alpha_{fH} f_H t)} \frac{k_H}{k_N} \quad t \neq 0, x = 0 \quad (56)$$

$$b_{2H}(0, 0) = 1 - \frac{f_H}{f_N} \frac{k_H}{k_N} \quad (57)$$

The band-stopping filters can be produced from the sum of the low- and high-pass filters, but are not given here for the sake of brevity.

### Two-dimensional radially symmetric filters

In many geological and geophysical investigation techniques (for example of gravity and magnetic methods), data are only dependent on spatial coordinates, with the two orthogonal coordinates such as the  $x$ -axis and  $y$ -axis in distance defining the space domain. The domain of Fourier transformed data is spatial frequency (wavenumber) ( $k_x - k_y$  or  $u-v$ ) and has a dimension defined by the number of cycles per unit distance. Such filters are usually designed as radially symmetric, so that the cutoff wavenumber becomes independent of direction. The wavenumber response of a 2D radially symmetric low-pass filter can be derived from the corresponding 1D filter (equation 1) by substituting frequency ( $f$ ) with the variable  $k = \sqrt{k_x^2 + k_y^2}$ :

$$H_{RL}(k) = \frac{1}{2} \left\{ \tanh \left[ \frac{2(k + k_L)}{r_L} \right] - \tanh \left[ \frac{2(k - k_L)}{r_L} \right] \right\} \quad (58)$$

where  $k_L$  and  $r_L$  denote the cutoff wavenumber and the half-width of the transition-band (see Figure 5e). Using equation (2), the filter spectrum can be written as follows:

$$B_{RL}(k) = \frac{\Delta x \Delta y}{2} \left\{ \tanh \left[ \frac{2(k + k_L)}{r_L} \right] - \tanh \left[ \frac{2(k - k_L)}{r_L} \right] \right\} \quad (59)$$

In a similar way, the other 2D symmetric wavenumber responses can be derived from their 1D counterparts via the same operation through equations (9), (14) and (19), respectively. In the wavenumber domain, the filtering operation is carried out via the multiplication of the filter spectrum by the Fourier transform of the data. The inverse Fourier transform then yields the filtered data in the distance domain.

The following Hankel transform pair connects the low-pass wavenumber response function to the corresponding impulse response function and vice-versa:

$$H(k) = 2\pi \int_0^{\infty} h(r) J_0(2\pi kr) r dr \quad (60)$$

$$h(r) = 2\pi \int_0^{\infty} H(k) J_0(2\pi kr) k dk \quad (61)$$

where  $J_0$  is the zero-order Bessel function of the first kind and  $r = \sqrt{x^2 + y^2}$ . The above pair is derived from the properties of the two-dimensional Fourier transform of radially symmetric functions (e.g. Buttkus, 2000). Accordingly, the filter coefficient in the distance domain can be calculated as

$$b(r) = 2\pi \int_0^{\infty} B(k) J_0(2\pi kr) k dk \quad (62)$$

where

$$B(k) = B(k_x, k_y) = \Delta x \operatorname{rect}\left[\frac{1}{2\Delta x}\right] \Delta y \operatorname{rect}\left[\frac{1}{2\Delta y}\right] H(k) = \Delta x \Delta y H(k) \quad (63)$$

that yields

$$b_{RL}(r) = \pi \Delta x \Delta y \int_0^{\infty} \left\{ \tanh\left[\frac{2(k+k_L)}{r_L}\right] - \tanh\left[\frac{2(k-k_L)}{r_L}\right] \right\} J_0(2\pi kr) k dk \quad (64)$$

The value of the first HT function is always unity for positive values of the wavenumber, and accordingly equation (64) reduces to

$$b_{RL}(r) = \pi \Delta x \Delta y \int_0^{\infty} \left\{ 1 - \tanh\left[\frac{2(k-k_L)}{r_L}\right] \right\} J_0(2\pi kr) k dk \quad (65)$$

Finally, via the application of the rectangle rule of integration, the above integral can be substituted by the following sum:

$$b_{RL}(r) = \pi \Delta x \Delta y \Delta k \sum_{j=1}^{\infty} j \left\{ 1 - \tanh\left[\frac{2(j\Delta k - k_L)}{r_L}\right] \right\} J_0(2\pi r j \Delta k) \quad (66)$$

Since  $J_0(0) = 1$ , the numerical value of the coefficient at the centre of the filter (where  $r=0$ ) can be given as follows:

$$b_{RL}(0) = \pi \Delta x \Delta y \int_0^{\infty} \left\{ 1 - \tanh\left[\frac{2(k-k_L)}{r_L}\right] \right\} k dk \quad (67)$$

If the half-width of the transition zone ( $r_L$ ) approaches zero, then the limit of the HT window yields a rectangular function whose size is equal to  $2k_L$ , as shown in the Appendix (A11):

$$\lim_{r_L \rightarrow 0} \frac{1}{2} \left\{ 1 - \tanh\left[\frac{2(k-k_L)}{r_L}\right] \right\} = \operatorname{rect}(k_L).$$

This result leads to the easy determination of the desired value as follows:

$$b_{RL}(0) = 2\pi \Delta x \Delta y \int_0^{\infty} \operatorname{rect}(k_L) k dk$$

$$b_{RL}(0) = 2\pi \Delta x \Delta y \int_0^{k_L} k dk = \pi \Delta x \Delta y k_L^2 = \frac{\pi k_L^2}{4k_{Nx}k_{Ny}} \quad (68)$$

where  $k_{Nx}$  and  $k_{Ny}$  are the values of Nyquist wavenumbers corresponding to the  $x$  and  $y$  variables, respectively. After determining the filter spectrum of a low-pass filter in the wavenumber domain, a band-pass filter spectrum (see Figure 5f) can be derived from the subtraction of two low-pass filters from each other:

$$B_{RB}(k) = \Delta x \Delta y [H_L(k, k_H) - H_L(k, k_L)] \quad (69)$$

Substitution of equation (65) into (69) for the high- ( $k_H$ ) and low-end ( $k_L$ ) wavenumbers of the filter pass-band, respectively, yields

$$B_{RB}(k) = \frac{\Delta x \Delta y}{2} \left\{ \tanh\left[\frac{2(k-k_H)}{r_H}\right] - \tanh\left[\frac{2(k-k_L)}{r_L}\right] \right\} \quad (70)$$

Consequently, the filter coefficients can be calculated from the following integral equation:

$$b_{RB}(r) = \pi \Delta x \Delta y \int_0^{\infty} \left\{ \tanh\left[\frac{2(k-k_H)}{r_H}\right] - \tanh\left[\frac{2(k-k_L)}{r_L}\right] \right\} J_0(2\pi kr) k dk \quad (71)$$

The numerical value of the filter coefficients at the centre of the filter can be determined with the help of (68) in the same way:

$$b_{RB}(0) = \pi \Delta x \Delta y (k_H^2 - k_L^2) = \frac{\pi(k_H^2 - k_L^2)}{4k_{Nx}k_{Ny}} \quad (72)$$

The wavenumber response of a high-pass filter (see Figure 5g) and spectrum can be derived in the conventional way used for one-dimensional cases:

$$H_{RH}(k) = 1 - H_{RL}(k, k_H) \quad (73)$$

$$B_{RH}(k) = \Delta x \text{rect}(k_{Nx}) \Delta y \text{rect}(k_{Ny}) [1 - H_{RL}(k, k_H)] \quad (74)$$

After algebraic manipulation, the wavenumber response of the high-pass filter becomes

$$B_{RH}(k) = \Delta x \text{rect}(k_{Nx}) \Delta y \text{rect}(k_{Ny}) - \Delta x \Delta y \frac{1}{2} \left\{ \tanh \left[ \frac{2(k + k_H)}{r_H} \right] - \tanh \left[ \frac{2(k - k_H)}{r_H} \right] \right\} \quad (75)$$

In order to derive an expression for the filter coefficients in the distance domain, the two-dimensional Fourier transform has to be applied to the above equation. The transform of the first term produces the following pair:

$$\Delta x \frac{\sin(2\pi k_{Nx}x)}{\pi x} \Delta y \frac{\sin(2\pi k_{Ny}y)}{\pi y} \leftrightarrow \Delta x \text{rect}(k_{Nx}) \Delta y \text{rect}(k_{Ny}) \quad (76)$$

The second term can be evaluated by the Hankel transformation, accordingly the filter coefficients in the distance domain can be given as:

$$b_{RH}(r) = \frac{\sin(2\pi k_{Nx}x)}{2\pi k_{Nx}x} \frac{\sin(2\pi k_{Ny}y)}{2\pi k_{Ny}y} - \pi \Delta x \Delta y \int_0^\infty \left\{ \tanh \left[ \frac{2(k + k_H)}{r_H} \right] - \tanh \left[ \frac{2(k - k_H)}{r_H} \right] \right\} J_0(2\pi kr) k dk \quad (77)$$

Since the first term is always zero, except for  $x=0$ ;  $y=0$ , and the first HT in the integral is always equal to one for positive values of the

variable  $k$ , the above equation can be simplified to

$$b_{RH}(r) = -\pi \Delta x \Delta y \int_0^\infty \left\{ 1 - \tanh \left[ \frac{2(k - k_H)}{r_H} \right] \right\} J_0(2\pi kr) k dk \quad (78)$$

The filter coefficients at particular points are

$$b_{RH}(x=0, y) = \frac{\sin(2\pi k_{Ny}y)}{2\pi k_{Ny}y} - \pi \Delta x \Delta y \int_0^\infty \left\{ 1 - \tanh \left[ \frac{2(k - k_H)}{r_H} \right] \right\} J_0(2\pi kr) k dk \quad (79)$$

$$b_{RH}(x, y=0) = \frac{\sin(2\pi k_{Nx}x)}{2\pi k_{Nx}x} - \pi \Delta x \Delta y \int_0^\infty \left\{ 1 - \tanh \left[ \frac{2(k - k_H)}{r_H} \right] \right\} J_0(2\pi kr) k dk \quad (80)$$

$$b_{RH}(0,0) = 1 - 2\pi \Delta x \Delta y \int_0^{k_H} k dk = 1 - \pi \Delta x \Delta y k_H^2 = 1 - \frac{\pi k_H^2}{4k_{Nx}k_{Ny}} \quad (81)$$

Any band-stopping filter (see Figure 5h) can be constructed by the summation of low- and high-pass filters. The summation of equations (63) and (77) yields, after some simplification taking into account the properties of the HT function, the following expression:

$$B_{RS}(k) = \Delta x \text{rect}(k_{Nx}) \Delta y \text{rect}(k_{Ny}) + \frac{\Delta x \Delta y}{2} \left\{ \tanh \left[ \frac{2(k - k_H)}{r_H} \right] - \tanh \left[ \frac{2(k - k_L)}{r_L} \right] \right\} \quad (82)$$

The inverse Fourier transformation of the above equation provides the time domain expression that serves in the calculation of filter coefficients:

$$b_{RS}(r) = \frac{\sin(2\pi k_{Nx}x)}{2\pi k_{Nx}x} \frac{\sin(2\pi k_{Ny}y)}{2\pi k_{Ny}y} + I_r \quad (83)$$

where

$$I_r = \pi \Delta x \Delta y \int_0^\infty \left\{ \tanh \left[ \frac{2(k - k_H)}{r_H} \right] - \tanh \left[ \frac{2(k - k_L)}{r_L} \right] \right\} J_0(2\pi kr) k dk$$

Some points require special care and hence the following equations should be applied in the calculation of the filter coefficients:

$$b_{RS}(r) = I_r \quad x \neq 0, y \neq 0 \quad (84)$$

$$b_{RS}(x=0, y) = \frac{\sin(2\pi k_{Ny} y)}{2\pi k_{Ny} y} + I_r \quad (85)$$

$$b_{RS}(x, y=0) = \frac{\sin(2\pi k_{Nx} x)}{2\pi k_{Nx} x} + I_r \quad (86)$$

The value of the filter coefficient at the centre can be obtained by the summation of (68) and (81):

$$b_{RS}(0,0) = 1 - \frac{\pi(k_H^2 - k_L^2)}{4k_{Nx}k_{Ny}} = 1 - \pi\Delta x\Delta y(k_H^2 - k_L^2) \quad (87)$$

### APPLICATION EXAMPLES

The computer programs that are used to produce the examples given here as well as supplementary materials consisting of several examples, data files and an instruction file can be requested from the author. The programs are written in PV-WAVE (see <http://www.vni.com/>). Both measured and test data sets can be processed, and these make them useful both in professional and educational applications, respectively. The 1D computer programs *fr1D* and *tm1D* perform filtering operations in the frequency and time domains, respectively. The user can generate a test data set by using some signals, namely; a sum of sinusoidal functions, a serial combination of individual sinusoidal functions, a set of chirp signals and a vibroseis sweep. The frequency varies with time in the latter two signals. The filtering operation begins with the fast Fourier transform (FFT) of the data. The transformed data is multiplied by the filter spectrum in the frequency domain and then transformed back to the time domain by the inverse Fourier transform. The FFT algorithms use positive index numbers for the data points and thus compute the spectrum in the frequency range of zero to twice the Nyquist frequency. This is not problematic, since the calculated spectrum is periodic, with a period defined by the number of data points and sampling interval. However, the transformed data is shifted in the range of  $-f_N$  to  $f_N$ . Instead

of this procedure, the computer program *fr1D* calculates the filter spectrum in the range 0 to  $2f_N$  and directly multiplies it by the output of the FFT algorithm before proceeding with the inverse Fourier transform. The shifted filter spectrum of a low-pass 1D filter resembles a high-pass filter (see Figure 6a). Accordingly, it can be obtained from the subtraction from unity of a HT window whose cutoff frequencies equal  $f_L$  and  $2f_N - f_L$  (see equation (14) for comparison):

$$H_L(f) = 1 - \frac{1}{2} \left\{ \tanh \left[ \frac{2(f - f_L)}{r_L} \right] - \tanh \left[ \frac{2(f - 2f_N + f_L)}{r_L} \right] \right\} \quad (88)$$

Figure 6b illustrates an example of a band-pass filter whose spectrum can be obtained by the subtraction of two low-pass filters as follows:

$$H_B(f) = \frac{1}{2} \left\{ \begin{aligned} & \tanh \left[ \frac{2(f - f_L)}{r_L} \right] - \tanh \left[ \frac{2(f - 2f_N + f_L)}{r_L} \right] \\ & - \tanh \left[ \frac{2(f - f_H)}{r_H} \right] + \tanh \left[ \frac{2(f - 2f_N + f_H)}{r_H} \right] \end{aligned} \right\} \quad (89)$$

The shifted spectrum of a high-pass filter (Figure 6c) is similar to the spectrum of a low-pass filter with cutoff frequencies  $f_H$  and  $2f_N - f_H$ :

$$H_H(f) = \frac{1}{2} \left\{ \tanh \left[ \frac{2(f - f_H)}{r_H} \right] - \tanh \left[ \frac{2(f - 2f_N + f_H)}{r_H} \right] \right\} \quad (90)$$

Finally, the shifted spectrum of a band-stopping filter (Figure 6d) can be obtained from the combination of the shifted low- and high-pass filters. Some examples demonstrating the application of the above-mentioned filters with the help of test data produced from the summation and combination of sinusoidal functions, chip signal and vibroseis sweep, are provided in the supplementary material. The computer program *tm1D* performs equivalent operations in the time domain. Since multiplication in the frequency domain is equivalent to convolution in the space or time domain, convolution of the input data by filter coefficients produces the

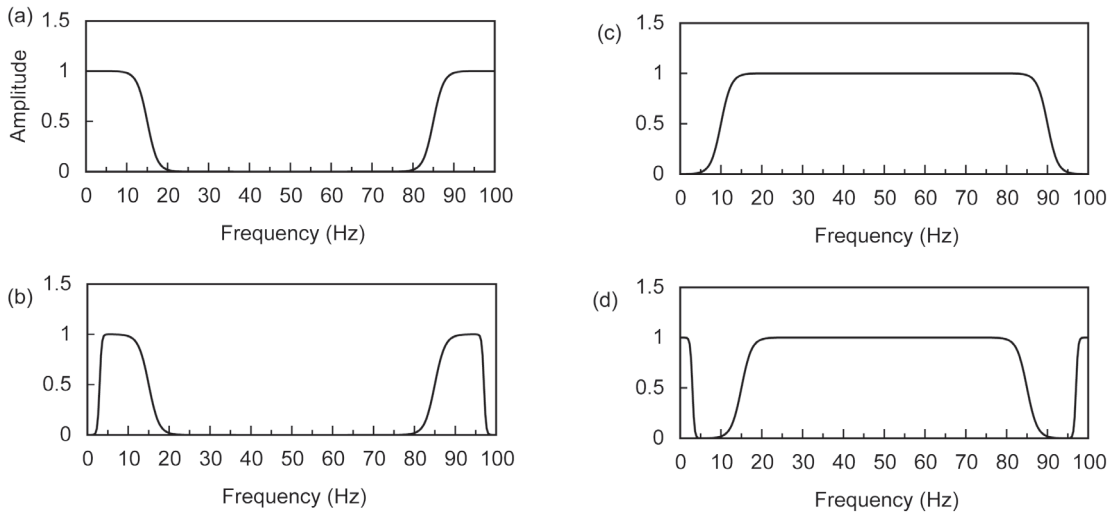


Figure 6. Shifted frequency responses of one-dimensional low- (a), band- (b), high-pass (c) and band-stopping filters. The frequency axis is limited to between zero and twice the Nyquist frequency.

Şekil 6. Bir-boyutlu alçak- (a), aralık- (b), yüksek-geçişli (c) ve aralık-durdurucu süzgeçler için kaymış frekans bölgeyi yanıtı. Frekans eksenini sıfır ile Nyquist frekansının iki katı arasında sınırlandırılmıştır.

desired output. Any 1D filter must exist in both the positive and negative time direction and the number of filter coefficients must be odd to satisfy the symmetry condition, or a time shift will occur in the output data. Moreover, in order not to cause amplitude distortion, the sum of the filter coefficients should be equal to (or at least be very close to) unity for the low-pass and band-stopping filters, and it should be equal to zero for the band- and high-pass filters. The value of this sum is established via the use of an input function consisting of a series of equally spaced samples representing a constant, which has a zero frequency component in the frequency domain. In this case, the low-pass and band-stopping filters should pass these constants without any change, while the output of the band- and high-pass filters must be equal to zero. The individual values of each filter coefficient versus time can be computed using the corresponding time domain expressions of (6), (12), (17) and (24). The limiting values of the filter coefficients at the centre of the filters are given in equations (8), (13), (18) and (23), respectively. The amount of output data will be less than that of input data in the time domain filtering. The digital filtering operation

commences with the matching of the filter and input data at the initial abscissa values. The sum of the products of the corresponding sample values of the filter and input data produces the first output sample value. The abscissa value of the first output sample is equal to the abscissa value of the input datum multiplied by the central filter coefficient. Consequently, the length of the output data will be shortened with filter length, namely by half of the length between the beginning and end parts of the input data. For this reason, the filtering operation should preferably be performed in the frequency domain - except in those cases where computational cost becomes a significant factor.

Four computer programs; *b2d-fr*, *b2d-tm*, *r2d-fr* and *r2d-tm* employ two-dimensional box-shaped (first character *b*) and radially symmetric filters (first character *r*) in both the frequency and time domains (ending with *fr* and *tm*, respectively). The frequency responses of these filters have already been illustrated in Figure 5. These programs read measured data in the three column *xyz* file format, as well as being used to create test data sets. There is also the option of saving both the original and filtered data in spreadsheet format. The following

expressions were used for the production of test data sets:

$$z(r) = e^{-\alpha r} [a \cos(f_1 r) + b \sin(f_2 r)] \quad (91)$$

$$z(r) = e^{-\alpha r} [a \cos(f_1 x) + b \sin(f_2 y)] \quad (92)$$

$$z(r) = e^{-\alpha r} [a \cos(f_1 x) b \sin(f_2 y)] \quad (93)$$

where

$r = \sqrt{x^2 + y^2}$ .  $f_1, f_2$  and  $a, b$  are the frequencies and amplitudes of cosine and sinus functions, respectively. The first function defines the sum of two circular sinusoidal functions. In the second and third expressions, the cosine and sinus functions are dependent on either variable  $x$  or  $y$ , defining a sum or multiplication of two perpendicular sinusoidal functions, respectively. The amplitude of a sinusoidal function is attenuated depending on the coefficient ( $\alpha$ ) of the radially symmetric exponential function. Zero values result in no attenuation. The direction of the sinusoidal function with respect to coordinate axis can be rotated in (92) and (93), but this is not necessary for equation (91) since it produces a radially symmetric data set.

Figure 7 illustrates an example of the 2D digital filtering operation. The test data were produced by the use of (92). Two perpendicular sinusoidal functions oscillating at frequencies of 5 and 15 Hz were combined to construct a test data set (see Figure 7a). In order to apply a slight attenuation, the coefficient of the exponential function was chosen to be equal to unity. A low-pass box-shaped filter whose cutoff frequency and half-width were equal to 7 and 2 Hz, respectively, was applied to this data set in the frequency domain. The corresponding output in the time domain was obtained by the inverse Fourier transform, and is illustrated in Figure 7b. The directional sinusoidal function oscillating at 15 Hz is completely suppressed while the 5 Hz sinusoidal function perpendicular to the former remains in the data set.

## CONCLUSIONS

It has been shown that the signum and unit step functions, and consequently the rectangular function, can be defined by a combination of HT functions. These definitions lead to frequency response functions that are analytical in whole space from  $-\infty$  to  $+\infty$  without any discontinuity. The suggested HT windows provide an opportunity to precisely adjust the transition band of the frequency response function. In view of the definitions provided in this paper, any ideal filter can be considered as a limiting case of the corresponding HT filter. The related filter function in the time domain can be derived analytically from the frequency domain expressions, except radially symmetric two-dimensional filters. Since the time domain filter parameters are directly related to the frequency domain (for example, the half-width of the transition band), the user can easily adjust the filter coefficients in the time domain by imagining the frequency response function. The suggested filters permit the construction of a relatively short filter in the time domain, since the ripples of the response function can be suppressed by controlling the value of the half-width of the transition band.

Other types of filter can also be potentially designed by using the basic filters provided here. For example, a notch filter that removes noise at a particular frequency instead of a frequency band, can be constructed by narrowing the stopband of a band-stopping filter. This can be realized in such a way that the terminating frequency of the low passband is made equal to the starting frequency of the high passband. Consequently, the terminating frequency of the filter passband becomes equal to the low-end frequency plus the half-width of the transition band. Similarly, the starting frequency of the succeeding passband becomes equal to the high-end frequency of the filter stopband minus the half-width of the subsequent transition band.

## APPENDIX A. BASIC DEFINITIONS

The frequency reject filters are constructed using appropriate window functions that acts as

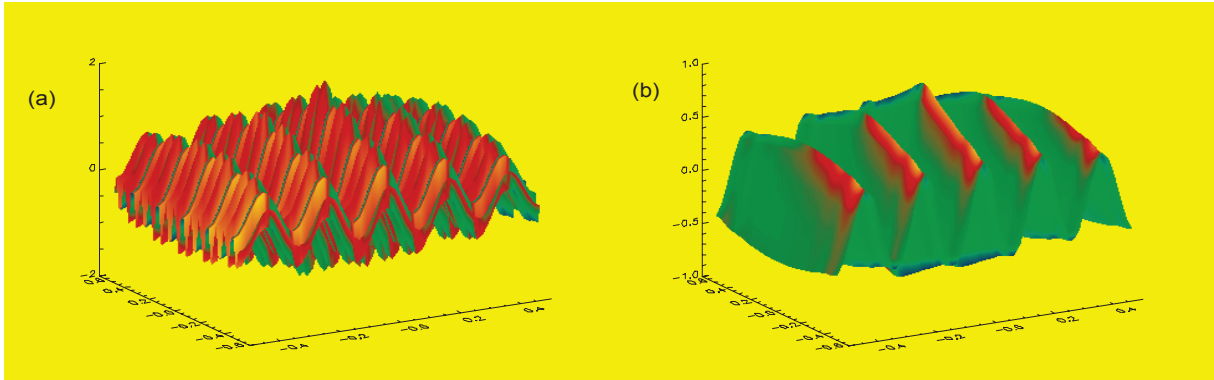


Figure 7. Low-pass filtering of a test data set (upper panel) consisting of two perpendicular sinusoidal functions (5 and 15 Hz). The high frequency sinusoidal is suppressed as a result of frequency domain filtering carried by a box-shaped frequency response function. The cutoff frequency and half-width are equal to 7 and 2 Hz, respectively.

Şekil 7. Birbirine dik iki sinüzoidalın (5 ve 15 Hz) toplamından oluşturulan deneme verisine (üstte) alçak-geçişli süzgeç uygulaması. Kutu-biçimli frekans yanıt fonksiyonu ile gerçekleştirilen frekans bölgesi süzgeçleme sonucunda yüksek frekanslı sinüzoidal bastırılmıştır. Kesme frekansı ve yarı-genişlik değerleri 7 ve 2 Hz değerlerine eşittir.

substitutes for the role of the rectangular function in the ideal filters. The rectangular function can be derived either from a self combination of signum or unit step functions. For this reason, definitions and Fourier transforms of the signum and unit step functions will be introduced using certain properties of the HT function. This permits the definition of the rectangular function as the summation of two shifted HT functions.

### A1. Definition and Fourier transform of the signum function

The following form of the HT function is used in this paper:

$$\tanh\left[\frac{\beta x}{r}\right] \quad (\text{A1})$$

where  $x$  is an independent variable that may represent time, distance, frequency etc. The HT function becomes equal to zero and unity when its argument is zero and greater than 5, respectively. In connection with this behaviour,  $r$  denotes the approximate length of the transition from zero to unity, with the total transition from -1 to 1 about  $2r$ .  $\beta$  is a constant

that defines the degree of approximation to unity at the point  $x=r$ . The percent relative error in the approximation can then be estimated as follows  $[1 - \tanh(\beta)]100\%$ . (A2)

For example, the percent relative errors for  $\beta = 2$  and  $\beta = 3$  are % 3.6 and % 0.5, respectively. Although the latter seems a better approximation, the selection of  $\beta = 2$  is a compromise between a good approximation to unity and the exhibition of well behaviour around  $x=r$  in view of the linear filter theory. The width of the transition becomes narrower as the value of  $r$  decreases. Hence the limit of the HT function approaches the signum function as  $r$  approaches zero:

$$\lim_{r \rightarrow 0} \tanh\left[\frac{\beta x}{r}\right] = \text{signum}(x) = \begin{cases} -1, & x < 0 \\ 0, & x = 0 \\ 1, & x > 0 \end{cases} \quad (\text{A3})$$

The Fourier transform of the signum function can also be obtained from the above property. The Fourier transform of definition (A1) can be derived from the following transform pair given by Bracewell (1965, page 366):

$$\tanh(\pi x) \leftrightarrow \frac{-i}{\sinh(\pi f)} \quad (\text{A4})$$

with the application of the scaling property yielding

$$\tanh\left[\frac{\beta x}{r}\right] \leftrightarrow \frac{-i\pi}{\beta} \frac{r}{\sinh(\pi^2 r f / \beta)}, \quad (\text{A5})$$

where  $i = \sqrt{-1}$ ,  $f$  denotes frequency and the symbol  $\leftrightarrow$  represents a Fourier transform pair. Since the limit of the left-hand side of the transform pair approaches the signum function as  $r$  approaches zero, the limit of the right-hand side in the frequency domain, by the application of L'Hôpital's rule, then provides the Fourier transform of the signum function:

$$\lim_{r \rightarrow 0} \tanh\left[\frac{\beta x}{r}\right] = \text{signum}(x) \leftrightarrow \lim_{r \rightarrow 0} \frac{-i\pi}{\beta} \frac{r}{\sinh(\pi^2 r f / \beta)} = \frac{-i}{\pi f} \quad (\text{A6})$$

## A2. Definition and Fourier transform of the unit step function

The unit step function can be defined in terms of signum and HT functions as a result of definition (A3):

$$U(x) = \frac{1}{2} + \frac{1}{2} \text{signum}(x) = \frac{1}{2} + \frac{1}{2} \lim_{r \rightarrow 0} \tanh\left[\frac{\beta x}{r}\right] = \begin{cases} 0, & x < 0 \\ \frac{1}{2}, & x = 0 \\ 1, & x > 0 \end{cases} \quad (\text{A7})$$

In this case, the Fourier transform of the unit step function can be easily derived from (A6) as follows:

$$U(x) = \frac{1}{2} + \frac{1}{2} \text{signum}(x) \leftrightarrow \frac{1}{2} \delta(f) - \frac{i}{2\pi f} \quad (\text{A8})$$

since

$$1 \leftrightarrow \delta(f).$$

It is also possible to define the signum function in terms of unit step function:

$$\text{signum}(x) = U(x) - U(-x) = 2U(x) - 1, \quad (\text{A9})$$

where  $U(-x)$  denotes the negative unit step function defined in the range  $(-\infty; 0)$ . These results indicate that the unit step function can be defined, at first, from the HT function by using equation (A7), with the signum function then defined in terms of the unit step function. For this reason, both functions have equal importance in digital filter theory.

## A3. Definition and Fourier transform of the rectangular function

The rectangular function can be obtained from either two shifted signum or unit step functions:

$$\text{rect}(L) = \frac{1}{2} [\text{signum}(x+L) - \text{signum}(x-L)] = U(x+L) - U(x-L) \quad (\text{A10})$$

where  $L$  is the half width of the rectangular function. The amplitude of the rectangular function equals 0.5 at abscissa points  $x=-L$  and  $x=L$ . Furthermore, as a result of definitions (A3) and (A7), the rectangular function can be defined as the limiting case of the combination of two shifted HT functions where  $\beta = 2$ :

$$\lim_{r \rightarrow 0} P(x) = \text{rect}(L) = \begin{cases} 0, & |x| > L \\ \frac{1}{2}, & |x| = L \\ 1, & |x| < L \end{cases} \quad (\text{A11})$$

where

$$P(x) = \frac{1}{2} \left\{ \tanh\left[\frac{2(x+L)}{r}\right] - \tanh\left[\frac{2(x-L)}{r}\right] \right\} \quad (\text{A12})$$

The  $r$  constant gives a good approximation to the half-width of the transition of the  $P(x)$  function. However, the above form differs in parameterization from the previous window applied to frequency reject filters by Basokur (1998):

$$P(x) = \frac{1}{2} \left\{ \tanh \left[ \frac{\pi(x+L)}{2\alpha L} \right] - \tanh \left[ \frac{\pi(x-L)}{2\alpha L} \right] \right\} \quad (\text{A13})$$

where the constant ( $\alpha$ ) is known as the ‘smoothness parameter’, since it controls the slope of the transition. The window given by (A13) is a modified version of Johansen and Sorensen’s (1979) P-function. It should be noted that the width of the transition could not be directly estimated in advance by using the smoothness parameter of Johansen and Sorensen (1979).

The Fourier transform of (A12) can be derived from the application of the shift theorem to the Fourier transform pair given in equation (A5):

$$\frac{1}{2} \tanh \left[ \frac{2(x+L)}{r} \right] \leftrightarrow \frac{-i\pi}{4} \frac{r}{\sinh(\pi^2 r f / 2)} \exp(2\pi L f),$$

$$\frac{1}{2} \tanh \left[ \frac{2(x-L)}{r} \right] \leftrightarrow \frac{-i\pi}{4} \frac{r}{\sinh(\pi^2 r f / 2)} \exp(-2\pi L f)$$

since

$$f(x \mp L) \leftrightarrow F(f) \exp(\mp 2\pi L f). \quad (\text{A14})$$

The summation of both sides of the above equations and the use of the Euler definition produce the following result:

$$P(x) \leftrightarrow \frac{\pi r}{2} \frac{\sin(2\pi L f)}{\sinh(\pi^2 r f / 2)}. \quad (\text{A15})$$

Since the shape of the P-function resembles a box-car function for small values of  $r$ , the corresponding function in the frequency domain thus resembles a *sinc* function. This can be shown by substituting  $r = 4\alpha L / \pi$  into (A15), yielding

$$P(x) \leftrightarrow 2\alpha L \frac{\sin(2\pi L f)}{\sinh(2\pi\alpha L f)}. \quad (\text{A16})$$

The right-hand side of the above transform was referred to as the ‘*sinsh*’ function by Johansen and Sorensen (1979). Since  $\sinh(x) \cong x$  for

small arguments, if  $\alpha$  (and consequently  $r$ ) is sufficiently small then the Fourier transform of the rectangular function can be derived as follows:

$$\lim_{\alpha \rightarrow 0} P(x) = \text{rect}(L) \leftrightarrow \frac{\sin(2\pi L f)}{\pi f}. \quad (\text{A17})$$

## REFERENCES

- Baldwin, P.R., and Penczek, P. A., 2007. The Transform Class in SPARX and EMAN2, *Journal of Structural Biology*, 157, 250–261.
- Başokur, A. T., 1983. Transformation of resistivity sounding measurements obtained in one electrode configuration to another configuration by means of digital linear filtering. *Geophysical Prospecting*, 31, 649–663.
- Başokur, A. T., 1998. Digital filter design using the hyperbolic tangent functions. *Journal of the Balkan Geophysical Society*, 1, 14–18. (< [http://www.balkan-geophysoc.gr/online-journal/1998\\_V1/feb1998/feb98.htm](http://www.balkan-geophysoc.gr/online-journal/1998_V1/feb1998/feb98.htm) /> ).
- Bracewell, R., 1965. *The Fourier Transform and its Applications*. McGraw-Hill Book Co., New York.
- Buttkus, B., 2000. *Spectral Analysis and Filter Theory in Applied Geophysics*. Springer, Berlin.
- Christensen, N. B., 1990. Optimized fast Hankel transforms. *Geophysical Prospecting*, 38, 545–568.
- Domaradzka, J. A., and Carati, D., 2007a. A comparison of spectral sharp and smooth filters in the analysis of nonlinear interactions and energy transfer in turbulence. *Physics of Fluids*, 19, 085111.
- Domaradzka, J. A., and Carati, D., 2007b. An analysis of the energy transfer and the locality of nonlinear interactions in turbulence. *Physics of Fluids*, 19, 085112.
- Ghosh, D.P., 1971. The application of linear filter theory to the direct interpretation of geoelectrical resistivity sounding

- measurements. *Geophysical Prospecting*, 19, 192-217.
- Johansen, H. K., and Sorensen, K., 1979. Fast Hankel transforms. *Geophysical Prospecting*, 27, 876-901.
- Opalka, N., Brown, J., Lane, W.J., Twist, K-AF., and Landick, R., 2010. Complete Structural Model of *Escherichia coli* RNA Polymerase from a Hybrid Approach. *PLoS Biol*, 8(9), e1000483. doi:10.1371/journal.pbio.1000483.
- Sorensen, K.I., and Christensen, N.B., 1994. The fields from a finite electrical dipole-A new computational approach. *Geophysics*, 59, 864-880.